Clinical and Experimental Obstetrics & Gynecology

Clin. Exp. Obstet. Gynecol. **2023**; 50(4): 81
https://doi.org/10.31083/j.ceog5004081

Original Research

Computed Tomography–Galactography Virtual Endoscopy: A Better Imaging Method for the Diagnosis of Pathologic Nipple Discharge

Nan Ma[1,2], Jiang Zhu[1], Yawen Wang[1], Kai Zhang[1], Song Zhao[1], Yongfeng Liang[3], Yan Deng[3,*,†], Rong Ma[1,*,†]

[1]Department of Breast Surgery, Qilu Hospital of Shandong University, 250012 Jinan, Shandong, China
[2]Department of Pediatric Surgery, The Second Hospital of Shandong University, 250031 Jinan, Shandong, China
[3]Department of Radiology, Qilu Hospital of Shandong University, 250012 Jinan, Shandong, China
*Correspondence: dengyan614@126.com (Yan Deng); marongw2000@163.com (Rong Ma)
†These authors contributed equally.
Academic Editor: Ambrogio Pietro Londero
Submitted: 18 January 2023 Revised: 26 February 2023 Accepted: 1 March 2023 Published: 17 April 2023

Abstract

Background: The preoperative diagnosis of pathologic nipple discharge (PND) in clinical settings remains challenging. Computed tomography-galactography virtual endoscopy (CT-G VE) was used for the intracavity imaging of discharging lactiferous ducts in a three-dimensional space, and the diagnostic performance of CT-G VE was compared with that of ultrasonography and galactography. **Methods**: This study included 41 patients with single-orifice PND who underwent ultrasonography, galactography, and CT-G VE before surgery. The postoperative histopathologic results were regarded as the gold standard for diagnosis. Qualitative data were analyzed using Fisher's precision probability test. Receiver operating characteristic (ROC) curve analysis was performed for ultrasonography, galactography, and CT-G VE to evaluate their diagnostic performances for the detection of PND diseases. **Results**: CT-G VE provided clear intracavity images of the discharging lactiferous ducts. The results of CT-G VE could be divided into five categories: negative, polypoid-solitary, polypoid-multiple, combined, and superficial types. The types were related to the histopathologic results. The detection ability of CT-G VE for high-risk and malignant lesions was higher than that of ultrasonography ($p = 0.0056$) and galactography ($p = 0.0008$). The detection abilities of CT-G VE alone and CT-G VE combined with ultrasonography were comparable. The cut-off point for CT-G VE was the polypoid-solitary type. The average effective dose for a single patient undergoing both chest CT and CT-G VE at the same time was 1.66 ± 0.78 msV. **Conclusions**: The diagnostic performance of CT-G VE was better than that of ultrasonography and galactography in detecting high-risk and malignant lesions of PND. This study proposed a grading system to aid decision-making and communication between clinicians in clinical practice.

Keywords: pathologic nipple discharge; computed tomography; galactography; virtual endoscopy; ultrasonography

1. Introduction

Pathologic nipple discharge (PND), defined as spontaneous single-orifice nipple discharge, is the second most common reason for consultation among patients requiring breast surgery. Intraductal papillary tumors, ductal ectasia, cystic hyperplasia, and breast cancer are some of the conditions that can result in PND [1]. The preoperative diagnosis of PND in clinical practice is challenging. Computed tomography (CT) is the first-line diagnostic tool used for diagnosing solid tumors, and the advent of spiral CT has enabled faster scans in addition to providing a wider range of images. Moreover, it can be used to evaluate small tumors in three dimensions with an increased resolution. Multislice spiral CT has been used to evaluate breast tumors and the range of breast cancers [2–4]. However, CT is rarely used in the diagnosis of breast diseases due to the limitations of imaging and radiation doses. Virtual endoscopy is a noninvasive technique that visualize the interior of hollow organs. It enables the observation of areas that cannot be reached using an endoscope and facilitates quantitative measurements. Virtual endoscopy has been used to visualize the bronchi [5], colon [6], heart [7], blood vessels [8], and throat [9]. In this study, we performed intracavity imaging of discharging lactiferous ducts and visualized the lesions three-dimensionally by combining galactography with CT and virtual endoscopy technologies.

2. Materials and Methods

2.1 Patients and Clinical Data

Forty-one female patients with spontaneous single-orifice nipple discharge who underwent surgery at the Department of Breast Surgery of our hospital between September 2020 and May 2021 were included in this study. All patients underwent ultrasonography, galactography, and CT-galactography virtual endoscopy (CT-G VE) before surgery. Galactography was performed immediately after CT. A definite histopathologic diagnosis was made after the surgery. Patients who were pregnant or had a plan of conceiving within 3 months and those with severe mental diseases, poor image quality, and missing clinical data were

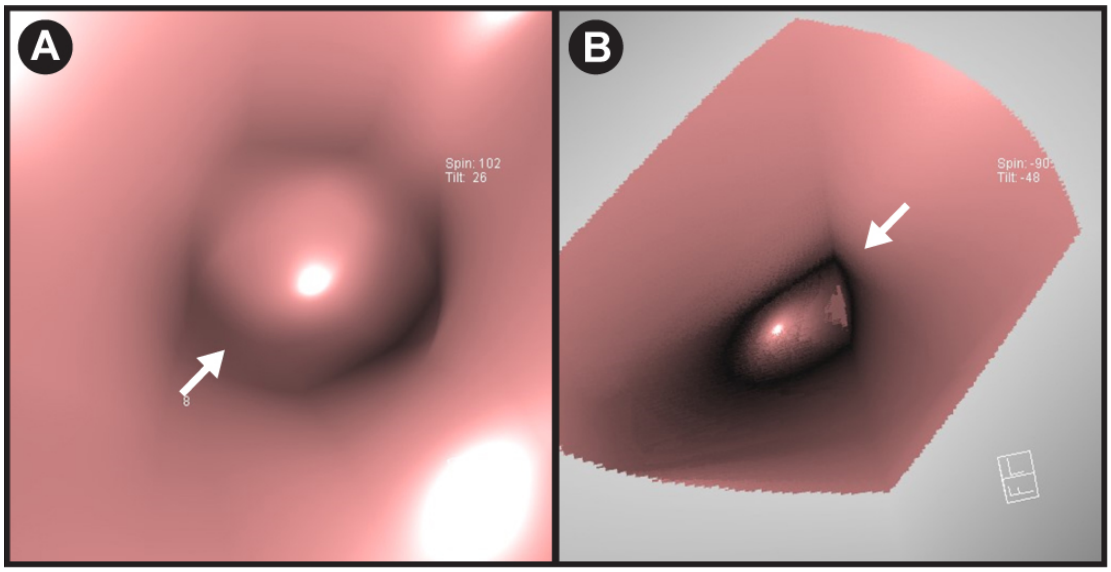

Fig. 1. Exemplary computed tomography-galactography virtual endoscopy (CT-G VE) images of the polypoid-solitary type (A, B).

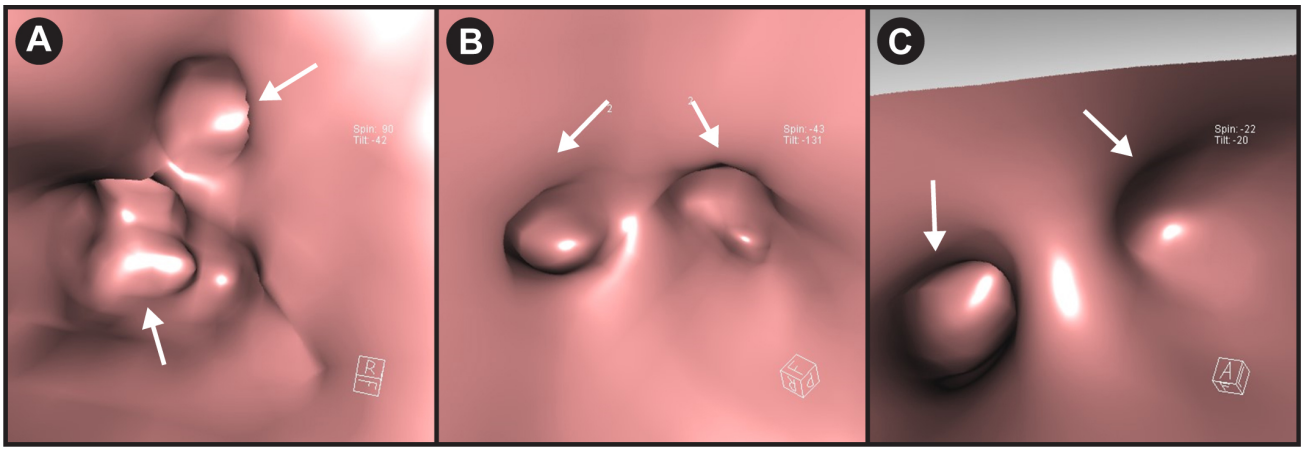

Fig. 2. Exemplary computed tomography-galactography virtual endoscopy (CT-G VE) images of the polypoid-multiple type (A, B, and C).

excluded. This study was approved by the local ethics committee, and written informed consent was obtained from all patients before participation.

2.2 Computed Tomography-Galactography Virtual Endoscopy

Before performing the examinations, 0.3–0.8 mL of ioversol was slowly injected into each target duct, which was discharged until the patient experienced mild pain or the contrast material overflowed. The injector was removed subsequently, and the breasts were cleaned gently.

All examinations were performed using a third-generation dual-source CT system (SOMATOM Force, Siemens Healthcare, Forchheim, Germany). The examinations were performed using automated tube current modulation (CAREDose4D, Siemens Healthcare, Forchheim, Germany) with a reference tube current time product of 130 mAs and automated attenuation-based tube voltage selection (CARE kV, Siemens Healthcare, Forchheim, Germany) with a reference tube potential of 120 kVp. The settings for the scanners were as follows: slice collimation of 192 $\times$ 0.6 mm employing a z-flying focal spot; gantry rotation time, 250 ms; pitch, 0.6; reformatted section thickness, 1.0 mm; and reformatted section increment, 1.0 mm. All patients were scanned craniocaudally in the supine position, with the arms positioned above the head. The whole chest was scanned from the superior aperture of the thorax to the inferior edge of the costophrenic angle during a deep inspiratory breath hold such that the bilateral breasts and axillary areas were covered. The images were reconstructed subsequently with a small field of view and a medium smooth convolution kernel optimized for imaging.

The CT data were processed on a Syngo.via workstation (Syngo.via VB20A, Siemens Healthcare, Forchheim,

Table 1. Categories of CT-G VE.

Categories	Morphological characteristics of the lesions
Negative type	Nothing of the following to be found.
Polypoid-solitary type	A single localized expansive growth lesion in a lactiferous duct, which is often hemispherical, pedicled, or spherical.
Polypoid-multiple type	Two or more localized expansive growth lesions in the lactiferous ducts, which are often hemispherical, pedicled, or spherical.
Superficial type	Superficial diffuse lesions in the lactiferous ducts, such as continuous luminal irregularity, luminal stenosis, or rough luminal surface accompanied by no obvious polypoid type lesions.
Combined type	The polypoid and superficial types coexisting in the same breast.

Abbreviations: CT-G VE, Computed tomography-galactography virtual endoscopy.

Germany) using various post-processing software, such as those for multiplanar reconstruction, curved surface reconstruction, maximum intensity projection, minimum intensity projection, volume reconstruction, and a CT virtual endoscope (CTVE). The ducts were observed from the primary catheter with the CTVE step-by-step for any increase in the diameter, filling defects in the lumen, shape and number of lesions, blockage of the lumen, interruption of the contrast medium and shape of the broken end, and thickening and rigidity of the attached tube wall. Two trained radiologists scored the visibility of the lesions on the CT images until a consensus was reached for each patient.

No standard classification system for CT-G VE results is available at present; therefore, we classified the morphological characteristics of the lesions into five categories (Table 1) according to the endoscopic classification of intraductal breast lesions published by the Japan Association of Mammary Ductoscopy in 2002 [10]. These categories included negative, polypoid-solitary, polypoid-multiple, combined, and superficial lesion types (Table 1).

2.3 Data and Statistical Analyses

The results of the imaging studies and histopathologic features of all enrolled patients were statistically analyzed. The ultrasonography results were classified into six categories based on the American College of Radiology Breast Imaging Reporting and Data System (ACR BI-RADS) and recorded [11]. Since no standard classification for the results of galactography is available at present, we used the Galactogram Grading System reported by Jiang to classify them into three grades: grade I, low risk; grade II, moderate risk; and grade III, high risk [12]. The patients were divided into the benign, high-risk, and malignant groups according to their postoperative histopathologic characteristics, which were regarded as the gold standard for diagnosis. Benign lesions included apocrine metaplasia, sclerosing adenosis, fibroadenoma, and a single intraductal papilloma. High-risk lesions included multiple intraductal papillomas and atypical hyperplasia. Malignant lesions included all types of breast cancer. Benign lesions were included in the negative group, whereas high-risk and malignant lesions were included in the positive group. Qualitative data were analyzed using Fisher's precision probability test. Receiver operating characteristic (ROC) curve analysis was performed to calculate the sensitivity and specificity of ultrasonography, galactography, and CT-G VE, and the diagnostic performances of the three imaging modalities were evaluated using the area under the ROC curve (AUC). Data were analyzed using Statistical Package for Social Sciences (Version 25.0, IBM Corp., Armonk, NY, USA) and MedCalc for Windows (Version 20, MedCalc Software, Ostend, Belgium). Statistical significance was set at $p < 0.05$.

3. Results

This study included 46 breasts of 41 patients; five patients presented with bilateral nipple discharge. The median age was 47 (range, 35–80) years.

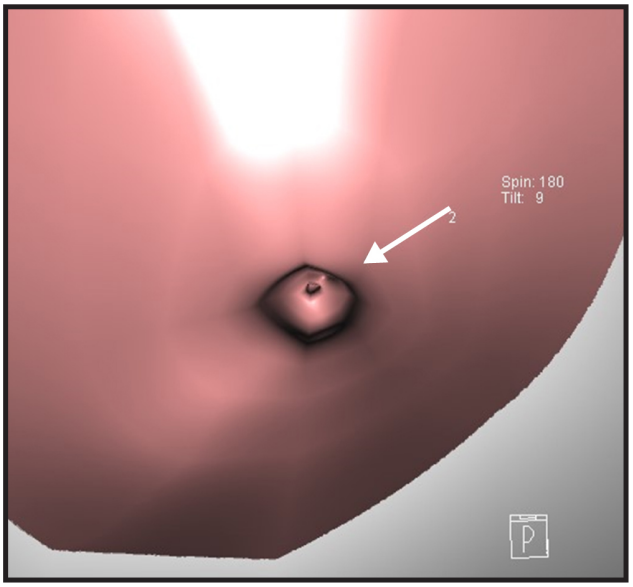

Fig. 3. Exemplary computed tomography-galactography virtual endoscopy (CT-G VE) image of the superficial type.

3.1 Histopathologic Correlations between the Results of the Three Imaging Modalities

Virtual endoscopy was performed with CT-galactography images to obtain intracavity images of the discharging lactiferous ducts. Typical images of the

Table 2. Imaging studies and pathological features.

Imaging modality			Number of breasts	Benign group	High-risk group	Malignant group	*p*
Ultrasonography	1		6	4	2	0	0.001
	2		4	1	2	1	
	3		11	5	6	0	
	4	4a	10	4	1	5	
		4b	9	0	3	6	
		4c	6	0	2	4	
	5		0	0	0	0	
	6		0	0	0	0	
Galactography	I		11	2	3	6	0.021
	II		23	11	9	3	
	III		12	1	4	7	
CT-G VE	Negative		7	6	0	1	0.000
	Polypoid-solitary		8	5	2	1	
	Polypoid-multiple		17	4	10	3	
	Superficial		1	0	0	1	
	Combined		13	0	3	10	

Abbreviations: CT-G VE, Computed tomography-galactography virtual endoscopy.

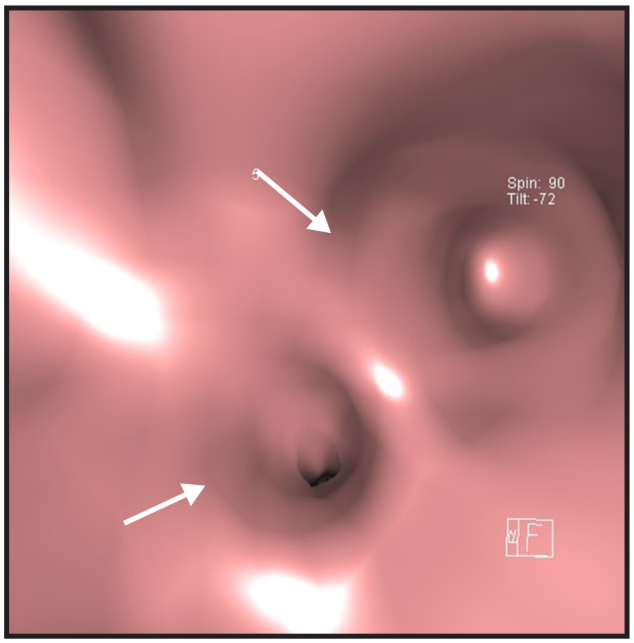

Fig. 4. Exemplary computed tomography-galactography virtual endoscopy (CT-G VE) image of the combined type.

polypoid-solitary (Fig. 1), polypoid-multiple (Fig. 2), superficial (Fig. 3), and combined type (Fig. 4) were obtained. The polypoid-multiple type was the most common type, followed by the combined type, whereas the superficial type was the rarest type. Table 2 presents the ultrasonography, mammography, and CT-G VE results of the benign, high-risk, and malignant lesions. Statistical analysis revealed histopathological correlations of the ultrasonography, galactography, and CT-G VE results.

3.2 Evaluation and Comparison of the Diagnostic Performance of the Three Imaging Modalities

ROC curve analysis (Tables 3,4 and Fig. 5) was performed for ultrasonography, galactography, and CT-G VE to evaluate the diagnostic performance of all three imaging modalities for PND diseases. The sensitivity for identifying high-risk and malignant lesions in PND was 64.52% [95% confidence interval (CI) 45.40–80.90%] for ultrasonography, 35.48% (95% CI 19.20–54.60%) for galactography, 87.10% (95% CI 70.20–96.40%) for CT-G VE, and 87.10% (95% CI 70.20–96.40%) for CT-G VE combined with ultrasonography. The specificity for identifying high-risk and malignant lesions in PND was 66.67% (95% CI 38.40–88.20%) for ultrasonography, 93.33% (95% CI 68.10–99.80%) for galactography, 73.33% (95% CI 44.90–92.20%) for CT-G VE, and 73.33% (95% CI 44.90–92.20%) for CT-G VE combined with ultrasonography. The AUC was 0.672 for ultrasonography, 0.588 for galactography, 0.876 for CT-G VE, and 0.885 for CT-G VE combined with ultrasonography. The detection ability of CT-G VE for high-risk and malignant lesions was higher than that of ultrasonography ($p = 0.0056$) and galactography ($p = 0.0008$). However, there was no significant difference between the detection abilities of ultrasonography and galactography ($p = 0.4780$). The detection abilities of CT-G VE alone and CT-G VE combined with ultrasonography were comparable ($p = 0.6412$). The cut-off point was the polypoid-solitary type for CT-G VE, category 3 for ultrasonography, and grade II for galactography.

3.3 Radiation Dose and Complications

The radiation doses were recorded and statistically analyzed. A single patient completed both chest CT and CT-G VE simultaneously; the average dose length product (DLP)

Table 3. ROC curve analysis of ultrasonography, galactography, CT-G VE, and CT-G VE combined with ultrasonography.

Imaging modality	Cut-off point	Sensitivity% (95% CI)	Specificity% (95% CI)	AUC (95% CI)	*p*
Ultrasonography	3	64.52 (45.40–80.90)	66.67 (38.40–88.20)	0.672 (0.518–0.803)	0.0360
Galactography	II	35.48 (19.20–54.60)	93.33 (68.10–99.80)	0.588 (0.433–0.731)	0.2461
CT-G VE	Polypoid-solitary type	87.10 (70.20–96.40)	73.33 (44.90–92.20)	0.876 (0.746–0.955)	<0.0001
CT-G VE combined with Ultrasonography		87.10 (70.20–96.40)	73.33 (44.90–92.20)	0.885 (0.756–0.960)	<0.0001

Abbreviations: ROC, Receiver operating characteristic; CT-G VE, Computed tomography-galactography virtual endoscopy; AUC, Area under the curve; CI, Confidence interval.

Table 4. Comparison of the AUC for ultrasonography, galactography, CT-G VE, and CT-G VE combined with ultrasonography.

Imaging modality	Difference in AUC	Z	*p*
Ultrasonography vs. galactography	0.0839	0.710	0.4780
CT-G VE vs. ultrasonography	0.204	2.772	0.0056
CT-G VE vs. galactography	0.288	3.345	0.0008
CT-G VE combined with ultrasonography vs. CT-G VE	0.00860	0.466	0.6412

Abbreviations: AUC, Area under the curve; CT-G VE, Computed tomography-galactography virtual endoscopy.

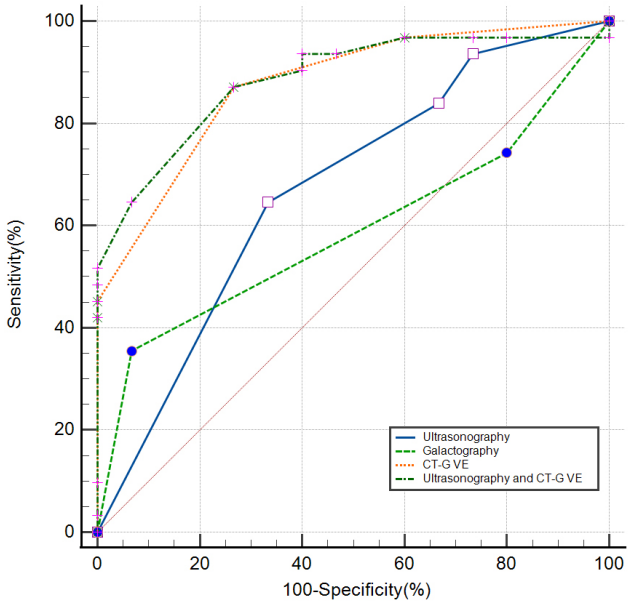

Fig. 5. Receiver operating characteristic (ROC) curves for the diagnostic performance of ultrasonography, galactography, computed tomography-galactography virtual endoscopy (CT-G VE), and CT-G VE combined with ultrasonography.

was 118.48 ± 55.48 mGy·cm, and the average effective dose was 1.66 ± 0.78 msV. 60.87% (28/46) patients experienced mild pain which was easily tolerated, while the others did not feel any pain. No serious complications, such as allergy to the contrast agent, infection, tissue necrosis, or bleeding, were observed in any of the patients following CT-G VE.

4. Discussion

PND is a common clinical manifestation in patients with heterogeneous breast diseases. These lesions are usually small, and their distribution is usually multicentric and multifocal along the affected lactiferous ducts [13]. Lesions within the same breast can be heterogeneous. Selective duct excision, a technique in which the glandular lobules where the discharging lactiferous ducts are located are removed completely, is the most commonly performed surgical method for PND currently. A histopathologic examination is performed, and the final resection scope is determined according to the histopathologic results. Owing to the comparatively lower accuracy for fast-frozen pathology in PND diseases, the rate of undergoing a second surgery is higher in PND diseases than in breast diseases with masses. Thus, preoperative localization and qualitative diagnosis play an important role in surgical planning.

The existing diagnostic methods for breast diseases have limitations when it comes to PND diseases [14,15]. Ultrasonography and galactography are often used as the first-line clinical imaging modalities for PND [1]. Ultrasonography can reveal dilated ducts and lesions within and outside the duct. However, this ability is greatly affected by the experience and capability of the examiners. Moreover, it is difficult to visualize the glandular tissue behind the nipple-areolar complex [16], and continuous visualization of the ductal system is not possible with ultrasonography. Galactography can only provide two-dimensional images, and accurate localization of the lesions is not possible as the breasts are squeezed during the imaging process. Pain caused by the squeezing of the breasts is the most common complaint. Small breasts cannot be imaged completely. Superposition of the breast tissue in patients with dense breasts

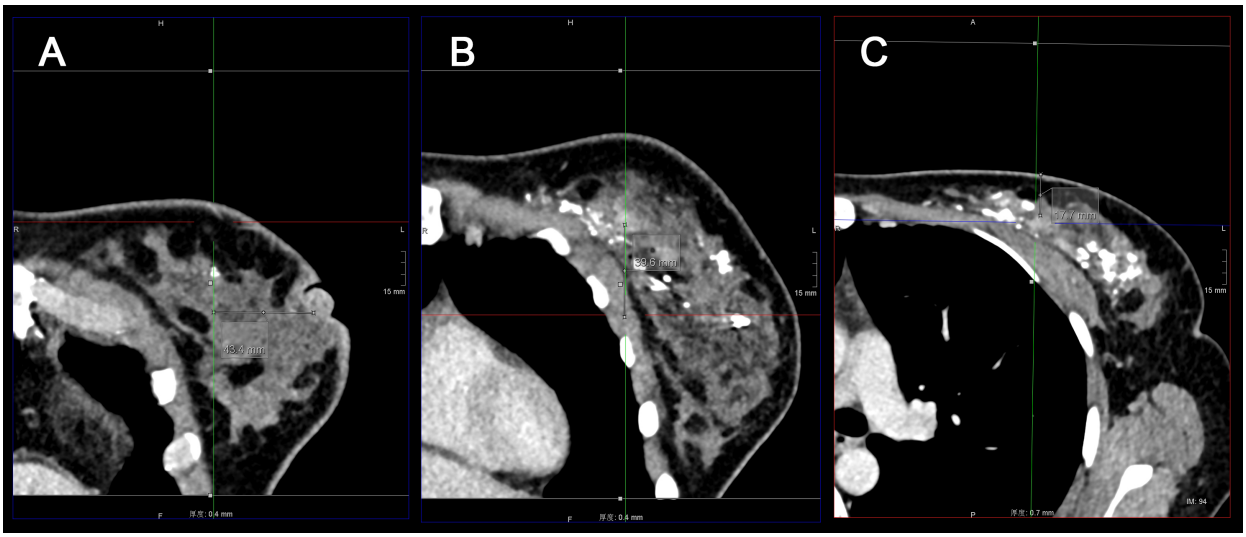

Fig. 6. Exemplary image of the accurate localization of a lesion using three-dimensional coordinates. (A) The horizontal distance from the lesion to the nipple. (B) The vertical distance from the lesion to the nipple. (C) The distance between the lesion and body surface.

reduces the sensitivity of X-rays [17,18].

The detection of breast disease by CT is limited by the sensitivity of the glandular tissue to ionizing radiation. However, the advantage of CT in assessing other solid tumors has prompted researchers to adapt it for breast diseases. Dedicated breast CT has been developed specifically for scanning breast. However, the localization of the lesions by dedicated breast CT can be inaccurate as the patient is in the prone position during scanning and supine position during surgery. Most dedicated breast CT imaging modalities require scanning of each breast to be performed individually with repositioning; this results in a longer scanning duration [19]. In 2001, Uematsu *et al*. [3] used three-dimensional helical CT to evaluate the scope of breast cancer lesions in guiding breast-conserving surgery. They proposed that helical CT could effectively detect intraductal and multicenter lesions in patients with breast cancer. In this study, we used a third-generation dual-source CT to scan the breasts and chest, thereby shortening the scanning. The average effective radiation dose for a single patient was controlled at 1.66 ± 0.78 msV, which was far less than that of a standard chest CT scan. However, the average effective radiation dose could be decreased further by reducing the scanning range such that only the breasts are being scanned. The abovementioned factors ensure the safety and rapidity of this examination. In addition, other diseases, such as lung lesions and aortic calcification, could be diagnosed simultaneously via the preoperative assessment.

In 2005, Matsuda proposed that spiral CT should be performed after galactography in patients with PND [20], as they considered it a useful method for visualizing tiny intraductal lesions by presenting the inner space of the duct using a virtual endoscopy technique. However, the initial findings need to be validated and summarized in more patients. Lesions in the ducts can be observed directly via ductography, which is an effective method for the diagnosis and treatment of PND. A meta-analysis including 36 studies and 3764 patients reported that ultrasonography and mammography were low-cost first-line diagnostic methods for patients with PND and that the performance of ductography was superior to that of other imaging techniques [21]. A meta-analysis including 10 studies and 894 patients reported that ductoscopy and magnetic resonance imaging (MRI) were equally sensitive in detecting malignant tumors in patients with PND; however, the specificity of ductoscopy was significantly higher than that of MRI [22]. The findings of the study by Ravza [23] also suggested that there was no statistical difference between the diagnostic performance of ductoscopy and that of MRI. CT-G VE can counter these shortages of real ductography. Virtual endoscopy is a three-dimensional reconstruction technique of spiral CT. Intraluminal imaging of the discharging ducts was performed by reconstructing the ducts using virtual endoscopy, thereby demonstrating that CT-galactography provided high-quality data for virtual endoscopy of the breast. It can be performed easily and is dispensed with special endoscopic instruments. Moreover, the mild pain associated with the procedure was easily tolerated by the patients. The ductoscopy could injury the duct and cause severe pain, bleeding, infection, or ductal shutting. Although there was no duct injury in our study, it is possible to puncture the openning of the duct with fail to recognize the target orifice and violent operations. Gentle and careful operations are very important. The ultimate goal of breast imaging is the early detection of breast cancer. Most imaging methods, such as ultrasonography and MRI, can identify a single lesion. In contrast, CT-galactography is more consistent with the disease progression of PND. The contrast agent fills the

target duct in a manner that is similar to the spread of the lesion along the affected duct, thereby enabling the marking of the extent of resection. CT-G VE can assess the morphological characteristics and boundaries of intraductal lesions easily and accurately, and parts of the invasive lesions outside the ducts could be observed to a certain degree. Tomographic and reconstructed images from CT-galactography have enabled three-dimensional observation of the lesions; thus, the positions of the lesions in the breast and anatomic relationships among multiple lesions could be observed simultaneously from the axial, sagittal, and coronal perspectives. This was a more intuitive and convenient solution for surgeons with limited experience in interpreting films, allowing them to perceive three-dimensional relationships "at a glance". The lesions should be positioned accurately using three-dimensional coordinates with the nipple as the origin to achieve refined treatment (Fig. 6). This maneuver aids in overcoming the limitations and inaccuracy associated with determining the location via ductoscopy. Accurate scopes, locations, and anatomic relationships of the lesions can be provided to surgeons, which can be applied to the preoperative simulation of surgical planning to achieve refinements in treatment. The detection ability of CT-G VE for high-risk and malignant lesions was higher than that of ultrasonography and galactography. In contrast, there was no significant difference in the diagnostic performance between CT-G VE and CT-G VE combined with ultrasonography, indicating that performing ultrasonography was not necessary when CT-G VE is performed. The cut-off points were the polypoid-solitary type for CT-G VE and category 3 for ultrasonography. These findings indicate the presence of high-risk or malignant lesions, even when imaging indicates a single or probably benign lesion. Moreover, they also confirmed that resection of a single lesion alone might not be a feasible surgical plan for patients with PND. In terms of radiation, CT-G VE could be a second-line diagnostic method for PND, while ultrasonography and galactography are the first-line diagnostic method. Due to its high sensitivity and excellent diagnostic performance, CT-G VE can be used for further diagnosis in patients with suspicious PND with negative ultrasonography and galactography results. Moreover, CT-G VE can exclude high-risk and malignant lesions ulteriorly in patients with PND pursuing clinical observation instead of surgery.

Theoretically, virtual endoscopy is feasible in every duct that can be filled with contrast material, and the observation range included the terminal duct beyond the narrow duct. Furthermore, the lesions can be observed from the periphery to the center and vice versa. Breast cancer is believed to originate from the terminal ductal lobular unit (TDLU). However, this area is difficult to image in the early stage of invasive diseases in humans unless excision and histopathologic examination are performed. In 2008, Ichihar *et al*. [24] visualized the three-dimensional structure of high-grade ductal carcinoma in situ and performed virtual ductoscopy using CT. This three-dimensional study obtained images that were almost equivalent to the low-power light microscopic view of the histological section. CT-G VE was able to visualize the structure of the TDLU and showed the intraductal and extraductal structural changes and features of lesions with high resolution, suggesting that it may enable the identification of lesions before the progression of the invasive disease. We aim to use CT-G VE to enhance our understanding of the development of breast cancer in patients presenting with PND by increasing the number of samples in subsequent studies, leading to an era of prediction and treatment of early breast cancer at lower costs for individuals and society.

The use of CT-galactography in clinical practice has several limitations presently. The examination cannot be performed in cases where the discharge cannot recur or the duct is exceedingly narrow due to difficulty in placing the injector. Furthermore, the distal duct cannot be detected if it is completely blocked by the lesions, resulting in a smaller range of lesions being detected than the true range. More effective indices for distinguishing between benign and malignant lesions are lacking.

Our study has some limitations. First, only a limited number of patients were enrolled in the study. We only enrolled patients who underwent surgery in this study to ensure that the histopathologic diagnosis was specific. Second, the diagnostic performance of MRI was not compared with that of CT-G VE. MRI requires a longer scanning time and is associated with higher costs, which few patients can afford. Moreover, patients with PND often have dilatated ducts filled with fluid, and the signals of fluid could mix with those of the lesions. Furthermore, a study of 111 patients with unilateral bloody nipple discharge concluded that MRI had limited diagnostic value in patients with negative ultrasonography and mammography findings [25]. Multimodal imaging of low-dose computed tomography-galactography provided intuitive images for surgical clinicians without requiring an understanding of the complex parameters of MRI. Lastly, accurate statistical analysis of the radiation doses of CT-G VE was not possible. All patients completed both chest CT and CT-G VE simultaneously as preoperative assessments. The radiation dose could potentially be reduced further if the scanning area is limited to the breasts.

5. Conclusions

In conclusion, intracavitary imaging of discharging ducts via a combination of galactography, CT, and virtual endoscopy techniques could provide abundant imaging data for the diagnosis of PND diseases. CT-G VE showed better diagnostic performance than ultrasonography and galactography in detecting high-risk and malignant lesions in PND. We proposed a grading system that would aid decision-making and communication between clinicians in clinical practice.

Abbreviations

PND, pathologic nipple discharge; CT, computed tomography; CT-G VE, CT-galactography virtual endoscopy; AUC, area under the curve; CTVE, CT virtual endoscope; DLP, dose length product; MRI, magnetic resonance imaging; ROC, receiver operating characteristic; TDLU, terminal ductal lobular unit.

Availability of Data and Materials

The raw data supporting the conclusions of this article will be made available by the authors, without undue reservation.

Author Contributions

RM and YD designed the research study. NM and JZ performed the research and wrote the manuscript. YW and SZ analyzed the data. KZ contributed to the interpretation of data and revised the manuscript critically for important intellectual content. YL contributed to the interpretation of data and the visualization and software. All authors contributed to editorial changes in the manuscript. All authors have participated sufficiently in the work and agreed to be accountable for all aspects of the work. All authors read and approved the final manuscript.

Ethics Approval and Consent to Participate

All subjects gave their informed consent for inclusion before they participated in the study. The experiments complied with the requirements of the Medical Ethics Committee of Qilu Hospital of Shandong University (No. KYLL-2-2111-139).

Acknowledgment

We thank Professor Yunyun Gong (School of Food Science and Nutrition, University of Leeds) for her guidance and suggestions for this article.

Funding

This work was supported by Shandong Provincial Natural Science Foundation (No. ZR2018MH029), Key Research and Development Program of Shandong Province, China (No. 2019GSF108058), Special Funds for Scientific Research on Breast Diseases of Shandong Medical Association (No. YXH2021ZX058), and Funding for New Clinical and Practical Techniques of Qilu Hospital of Shandong University (No. 2019-1).

Conflict of Interest

The authors declare no conflict of interest.

References

[1] Gupta D, Mendelson EB, Karst I. Nipple Discharge: Current Clinical and Imaging Evaluation. AJR. American Journal of Roentgenology. 2021; 216: 330–339.

[2] Perrone A, Lo Mele L, Sassi S, Marini M, Testaverde L, Izzo L, *et al*. MDCT of the breast. AJR. American Journal of Roentgenology. 2008; 190: 1644–1651.

[3] Uematsu T, Sano M, Homma K, Shiina M, Kobayashi S. Three-dimensional helical CT of the breast: accuracy for measuring extent of breast cancer candidates for breast conserving surgery. Breast Cancer Research and Treatment. 2001; 65: 249–257.

[4] Zhang X, Fu LP, Lan XQ, Sun LS, Li YS, Zhang YG, *et al*. Imaging post-processing technique in galactography with low-dose CT. Chinese Computed Medical Imaging. 2014; 20: 402–406.

[5] Moroni C, Bindi A, Cavigli E, Cozzi D, Luvarà S, Smorchkova O, *et al*. CT findings of non-neoplastic central airways diseases. Japanese Journal of Radiology. 2022; 40: 107–119.

[6] Kalra N, Gulati A, Gupta P, Dhaka N, Sehgal S, Singh S, *et al*. Comparison of virtual computed tomography enteroscopy using carbon dioxide with small-bowel enteroclysis and capsule endoscopy in patients with small-bowel tuberculosis. European Radiology. 2021; 31: 3297–3305.

[7] Yao LP, Zhang L, Mei J, Ding FB, Li HM, Ding M, *et al*. A pilot study of a cardiovascular virtual endoscopy system based on multi-detector computed tomography in diagnosing tetralogy of Fallot in pediatric patients. Experimental and Therapeutic Medicine. 2018; 15: 1552–1559.

[8] Wu PW, Tsay PK, Sun Z, Peng SJ, Lee CY, Hsu MY, *et al*. Added Value of Computed Tomography Virtual Intravascular Endoscopy in the Evaluation of Coronary Arteries with Stents or Plaques. Diagnostics. 2022; 12: 390.

[9] Guarnizo A, Glikstein R, Tsehmaister-Abitbul V, Busca I, El-Sayed S, Odell M. Comparison of diagnostic accuracy of computed tomography virtual endoscopy and flexible fibre-optic laryngoscopy in the evaluation of neck anatomic structures and neoplasms. The Neuroradiology Journal. 2021; 34: 8–12.

[10] Makita M, Akiyama F, Gomi N, Ikenaga M, Yoshimoto M, Kasumi F, *et al*. Endoscopic classification of intraductal lesions and histological diagnosis. Breast Cancer. 2002; 9: 220–225.

[11] Mendelson EB, Böhm-Vélez M, Berg WA, Whitman GJ, Feldman MI, Madjar H, *et al*. ACR BI-RADS Ultrasound. In: ACR BI-RADS Atlas, Breast Imaging Reporting and Data System. 2013. Available at: https://www.acr.org/-/media/ACR/Files/RADS/BI-RADS/US-Reporting.pdf (Accessed: 18 January 2023).

[12] Jiang L, Li X, Kong X, Ma T, Yang Q. Galactogram Grading System for Identifying Breast Cancer With Nipple Discharge. Clinical Breast Cancer. 2020; 20: e214–e219.

[13] Ohlinger R, Flieger C, Hahndorf W, Paepke S, Blohmer JU, Grunwald S, *et al*. Correlation of Ductoscopic and Histopathological Findings and Their Relevance as Predictors for Malignancy: A German Multicenter Study. Anticancer Research. 2020; 40: 2185–2190.

[14] Patel BK, Falcon S, Drukteinis J. Management of nipple discharge and the associated imaging findings. The American Journal of Medicine. 2015; 128: 353–360.

[15] Lee SJ, Trikha S, Moy L, Baron P, diFlorio RM, Green ED, *et al*. ACR Appropriateness Criteria® Evaluation of Nipple Discharge. Journal of the American College of Radiology. 2017; 14: S138–S153.

[16] Yoon JH, Yoon H, Kim EK, Moon HJ, Park YV, Kim MJ. Ultrasonographic evaluation of women with pathologic nipple discharge. Ultrasonography. 2017; 36: 310–320.

[17] Boyd NF, Guo H, Martin LJ, Sun L, Stone J, Fishell E, *et al*. Mammographic density and the risk and detection of breast cancer. The New England Journal of Medicine. 2007; 356: 227–236.

[18] Pisano ED, Gatsonis C, Hendrick E, Yaffe M, Baum JK, Acharyya S, *et al*. Diagnostic performance of digital versus film

mammography for breast-cancer screening. The New England Journal of Medicine. 2005; 353: 1773–1783.

[19] Zhu Y, O'Connell AM, Ma Y, Liu A, Li H, Zhang Y, *et al*. Dedicated breast CT: state of the art-Part I. Historical evolution and technical aspects. European Radiology. 2022; 32: 1579–1589.

[20] Matsuda M, Seki T, Kikawada Y, Isaka H, Teraoka H, Fukushima H, *et al*. Mammary ductoscopy by helical CT: initial experience. Breast Cancer. 2005; 12: 118–121.

[21] Filipe MD, Patuleia SIS, de Jong VMT, Vriens MR, van Diest PJ, Witkamp AJ. Network Meta-analysis for the Diagnostic Approach to Pathologic Nipple Discharge. Clinical Breast Cancer. 2020; 20: e723–e748.

[22] Filipe MD, Patuleia SIS, Vriens MR, van Diest PJ, Witkamp AJ. Meta-analysis and cost-effectiveness of ductoscopy, duct excision surgery and MRI for the diagnosis and treatment of patients with pathological nipple discharge. Breast Cancer Research and Treatment. 2021; 186: 285–293.

[23] Yılmaz R, Bender Ö, Çelik Yabul F, Dursun M, Tunacı M, Acunas G. Diagnosis of Nipple Discharge: Value of Magnetic Resonance Imaging and Ultrasonography in Comparison with Ductoscopy. Balkan Medical Journal. 2017; 34: 119–126.

[24] Ichihara S, Ando M, Maksimenko A, Yuasa T, Sugiyama H, Hashimoto E, *et al*. 3-D reconstruction and virtual ductoscopy of high-grade ductal carcinoma in situ of the breast with casting type calcifications using refraction-based X-ray CT. Virchows Archiv. 2008; 452: 41–47.

[25] van Gelder L, Bisschops RHC, Menke-Pluymers MBE, Westenend PJ, Plaisier PW. Magnetic resonance imaging in patients with unilateral bloody nipple discharge; useful when conventional diagnostics are negative? World Journal of Surgery. 2015; 39: 184–186.